Experimental study on bulge deformation of geotextile under ring-restrained conditions

Zhe Yang[1], Xia Xue[2], WangLin Li[3], Chen Li[4]
[1, 2]School of Water Conservancy and Environment, University of Jinan, Jinan, 250002, China
[4]Shandong Water Conservancy Engineering Test Center Co., Ltd., Jinan, 250013, China
[3]University of Jinan, Jinan, 250002, China
[3]Corresponding author
E-mail: [1]*zheyang98@qq.com*, [2]*xxhoper@163.com*, [3]*cswlwe@163.com*, [4]*1853595613@qq.com*

Received 7 November 2022; accepted 18 April 2023; published online 29 June 2023
DOI https://doi.org/10.21595/jme.2023.23042

Abstract. Geotextile layers are arranged on and below the geomembrane to prevent the geomembrane from being punctured and damaged. The geotextile not only plays a role in physical protection, like anti-puncture but also makes a great difference to the mechanical properties of the geomembrane's air expansion deformation. In this paper, the bulging deformation of geotextile is simplified as spherical bulging deformation under ring-restrained conditions. Using the special bulging deformation test equipment, the bulging deformation experiment of geotextile is realized, the main factors affecting the bulging deformation are analyzed, the law of bulging deformation and failure of geotextile is summarized, the failure mechanism of geotextile and the Influence of geotextile on the properties of geomembrane are discussed, and the following conclusions are drawn. The failure of bulging deformation of geotextiles belongs to tensile failure, which is characterized by fast speed and high strength. The typical failure mode is spindle-shaped cracks distributed along the crown, whose failure mechanism belongs to tensile failure produced in weak areas. The bulging deformation of the geotextile shows nonuniformity, with the largest deformation at the crown top and the smallest deformation at the ring constraint. When the geotextile is covered on the geomembrane, bulging pressure is shared by both the geomembrane and the geotextile. At the initial deformation stage, the geomembrane replaces it, and then the geotextile bears more internal pressure and plays a decisive role till destruction.

Keywords: anti-seepage of reservoir basin, geotextile, bulge deformation, influencing factors, tensile failure.

1. Introduction

As the regulating reservoir supporting project to the South-North Water Diversion Project, the Plain Reservoir, has taken on a more critical role since China's South-North Water Diversion Project has completed. In recent years, the northern region has begun to promote the anti-seepage technology of the reservoir basin with an all-spread geomembrane at the bottom of the reservoir in constructing the plain reservoir. Moreover, set a geotextile layer upon and beneath the geomembrane to prevent other objects from piercing and damaging the geomembrane. For plain reservoirs that use the anti-seepage with geomembranes, the change in air pressure distribution under the geomembranes which is caused by various factors, such as an increase in the groundwater level and the sudden drop in reservoir water level, will lead to the expansion or even damage of geomembranes [1].

According to previous studies, when studying the air expansion deformation properties of geomembranes, it is found that geotextile not only plays a physical protection role, like anti-puncture but also significantly impacts the air expansion mechanical properties of the geomembrane. In the research on the bulging deformation of horizontal impervious materials in plain reservoirs, there is little research on the mechanical properties of geotextile bulging deformation at present, and the related research is mainly embodied in geomembrane and composite geomembrane. Researchers conducted further research on composite geomembrane

and found that its geotextile plays a protective role and has an important impact on the overall mechanical properties [2-3]. In the process of bulging deformation and failure of composite geomembrane, when the lower geomembrane bulges and deforms, the upper geotextile also bulges and destroys simultaneously [4]. The enhancement effect of geotextile on geomembrane is obvious. Geotextile can improve the strength of composite materials and reduce the deformation rate, which has a certain effect on the mechanical characteristics of composite materials [5]. Other researchers have found that the rise of temperature that caused by solar radiation or lack of heat treatment affects tensile strength and meanwhile designed special multiaxial stretching equipment to study the real stress state of geosynthetics during stretching [6-9]. Merry and Bray [10-12] affirmed the true stress state under multiaxial tension and the spherical bulging deformation of geosynthetics under out-of-plane load and improved the stress-strain formula. Pan [13] studied the relationship between the strength and damage degree of geomembrane through experiments and obtained the laws of stress-strain and strength of different geomembranes after damage. The results showed that the geomembrane damage significantly influences the geomembrane's local stress-strain. Chu [14] concluded that the creep characteristic and fatigue life of geotextiles are closely related to the properties of the fiber material, microstructure, and cyclic loading conditions. For the determination of geotextile bursting properties, the existing standard is to measure the bursting performance of the specimen by the diaphragm bursting strength method [15, 16]. At present, the research on the mechanical properties of geotextiles is mainly through one-dimensional tensile test. However, geotextiles are mostly in a state of multi-axial stress in practical applications. Geotextile itself plays a protective role. This paper aims to explore how much pressure the geotextile can bear in the process of bulging and deformation and then analyze how much the geotextile enhances the geomembrane in the bulging and deformation process.

In this study, the developed geotextile bulging test equipment was used to regard the bulging deformation of geotextile as ring-restrained spherical deformation and explored influencing factors and mechanical characteristics of geotextile air expansion deformation. The spherical bulging deformation test cannot be performed under ring-restrained conditions because geotextile is a water and air permeability material. Therefore, it is necessary to use the water-tight and airproof polyethylene film cushion for experiments to obtain the bulging deformation mechanical properties of the geotextile.

Through the analysis of the failure characteristics of geotextile, the bulging deformation and failure mechanism of geotextile and the deformation characteristics of geotextile in different stages are clarified. At the same time, the protection and enhancement of the geotextile on bulging deformation are clarified compared with the geomembrane. In addition, the effects of mass per unit area and fiber type on the mechanical properties of geotextile bulging and deformation were also tested, which further enriched the research on the mechanical properties of bulging and deformation of geotextile and provided certain reference and guidance for engineering practice. Currently, geotextiles have been widely used in the horizontal anti-seepage system of plain reservoirs in the northern plains of China. Therefore, it is referential for practical design to study the mechanical properties of geotextile bulging deformation.

2. Test design

2.1. Test apparatus

This test was carried out at room temperature in the laboratory, using special test equipment designed by us to study the mechanical properties of bulging deformation under annular constraints. The model of the equipment is TSY-34A. TSY-34A tester for geomembrane bursting strength is developed and designed according to China's Specification for test and measurement of geosynthetics (SL/T235-2012) in geotechnical synthetic materials testing procedures. TSY-34A tester is suitable for measuring the bursting strength of various geosynthetic materials with stable performance and convenient use. The inner diameter of the sample restraint ring is

100 mm and 200 mm respectively. Currently, the relatively mature test standard is the American Multi-axial Tensile Test Standard for geosynthetic materials (ASTM) D 5617-04, but after research and analysis, When the ratio of the diameter of the fixture to the thickness of the film is more than 60, the relationship curves and distribution characteristics are the same, and there is no systematic difference. Therefore, according to the test sample index, the diameter of the test equipment is selected as 100 mm and 200 mm, and the ratio of the diameter of the fixture to the film thickness is 250, which meets the requirements.

Test equipment consists of three parts: a pressurization system, a control platform, and a measurement-control system, as shown in Fig. 1. The pressurization system includes a liquid pump and a hydro-cylinder; The control platform consists of a console, the operation platform, and the ring-restrained flange; The laser displacement sensor and pressure sensor constitute the measurement-control system. The materials used in each part of the equipment are as follows: For the liquid pump and hydro-cylinder in the pressurized system, their body is made of steel; The connecting pipeline uses hydraulic rubber hoses; The ring-restrained flange is made of stainless steel. The main body of the console and the operating platform is iron. The materials used for sensors and other auxiliary devices are not described in detail – no separate description for the equipment size. Only the flange diameter required for the test is explained.

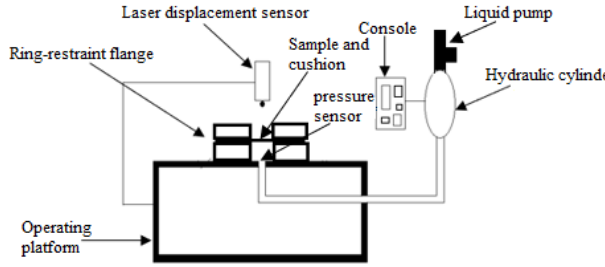

Fig. 1. Schematic diagram of test equipment

2.2. Test methods

Prepare the sample first, then check the operation of the equipment, and confirm whether the pressure sensor and laser displacement sensor are working correctly. Fill the hydro-cylinder with water, calibrate the displacement sensor and reset the pressure sensor. After that, press the start key of the program-controlled meter of the control platform until the sample is burst, which means the test ends. And finally collect the information and process the data. After the spherical bulging deformation test of the geotextile under ring-restrained was completed according to the above steps, the burst pressure P and burst crown height H during the test will be recorded. With reference to the American Society for Testing and Materials (ASTM) D 3786, calculate the bursting pressure of each specimen by subtracting the tare pressure required to inflate the diaphragm from the total pressure required to rupture the specimen. The tensile stress formula calculated the geotextile's tensile stress and strain, and the geotextile's characteristic curve could be obtained.

2.3. Test scheme

In order to study the influencing factors of bulging deformation, bulging deformation tests of the geotextiles were conducted with different material types and under different diameters and loading rates. Based on the selected diameters and loading rates, the American Society for Testing and Materials (ASTM) D 3786 suggests that a uniform pressure of 95±5 ml/min should be adopted. Consider of the approximate curve of bursting pressure and the diameters [17], seven loading rates (80, 90, 100, 110, 120, 130, 140 mL/min), two restraint flange diameters (inner diameter 100, 200 mm), and various material types (mass per unit area, fiber types, fiber lengths)

were used in the test in order to observe the bulging deformation obviously, as shown in Table 1. In addition, the geomembrane bulging test was added based on that of the geotextile to study the role that the geotextile plays when the geotextile and the geomembrane bulge together. Through on-site measurement, the initial thickness of geotextile with the same mass per unit area is slightly different, but it does not affect the study of its law. Therefore, the initial thickness is not processed as test data. This test aims to explore the characteristics of geotextile so the slight difference in initial thickness does not affect the overall mechanical properties of the sample. A specific test scheme is shown in Table 1, and Table 2 shows the common indicators of a needle-punched geotextile by the grab test.

Table 1. Test scheme

Experimental group/influencing factors	Loading rate, mL/min	Restraint flange diameter, mm	Material characteristics		
			Mass per unit area, g/m^2	Fiber type	Fiber length
1	80, 90, 100, 110, 120, 130, 140	200	300	Polyester fiber	Staple fibers
2	140	100, 200	200	Polyester fiber	Staple fibers
3	140	100	200	Polyester and polypropylene fiber	Staple fibers
4	140	100	200, 300, 400	Polyester fiber	Staple fibers
5	140	100	200	Polyester fiber	Staple fibers, filaments
6	140	200	250	Polyester fiber	Staple fibers

Table 2. Common indicators for a needle-punched geotextile

Fiber length	Mass per unit area, g/m^2	Strength at break, kN/m	Elongation at break, %	Tear strength, kN
Staple fibers/filaments	200	6.5/10.0	25~100/40~80	0.16/0.28
Staple fibers/filaments	300	9.5/15.0	25~100/40~80	0.24/0.42
Staple fibers/filaments	400	12.5/20.5	25~100/40~80	0.33/0.56

3. Test results and analysis

3.1. Geotextile bulge deformation failure characteristics and mechanism

3.1.1. Deformation and failure characteristics

Typical failure modes of geotextile spherical bulging deformation under ring-restrained conditions are shown in Fig. 2.

As can be seen from Fig. 2, the geotextiles will have tearing cracks after the destruction. At first, a crack is formed at the crown, then grows gradually along the crack until the sample bursts. Generally, the crack whose appearance is approximately spindle-shaped is located in the central area of the crown, and its trend is along the needle track formed by the needle punching reinforcement during the production process of the geotextile.

3.1.2. Deformation and failure mechanism

By analyzing the failure mechanism of the geotextile from the failure process, it is found that the stress concentration first occurs in a weak point of the geotextile, and then it is destroyed by

the stress concentration during the bulging deformation of the geotextile. As the test goes on, many fibers will detach and scatter in the transverse direction around the destruction place, and the cracks will continue to extend in the longitudinal direction and finally a spindle-like shape. Geotextiles are deformed uniformly in all directions. In multiple directions through the great circle curve, destruction co-occurs and additionally on any one great circle curve passing through the spherical cap, the tension force along the tangent direction is equal. Moreover, because the geotextile thickness at the spherical top is the thinnest, the tensile force along the curve's tangent is the largest. Put in another way, the tensile stress corresponding to the crown position is the largest.

a) b)

Fig. 2. Typical failure modes of geotextiles

The concentrated tensile stress makes the elongation in any weak area at the crown of geotextiles increase sharply. Meanwhile, the cross-section of the sample is significantly reduced in the weak area. That is the reason why it will form stress concentration that destroyed the geotextile. Therefore, the first damaged area is usually the crown of geotextiles. The geotextiles near the flange are also stretched due to the restrained ring, but the stretching degree at the ring constraint is far less severe than that at the crown because of the large restraint effect so no damage occurred. The bulging failure mode is presented as a shuttle shape passing through the top of the spherical crown or not. The failure mechanism is that under the action of liquid expansion, the fiber nodes in the needle punching direction of the local weak area of the crown detach failure, and the fiber perpendicular to the needle punching direction tears, the tensile failure caused by a chain reaction in low strength zone of fiber.

3.2. Stress-strain relationship of geotextile bulge deformation

The test process and the deformation and failure characteristics of geotextiles showed that the measurement of geotextile thickness t is complicated during the test. The thickness of the geotextile could not be accurately measured under restrained conditions, so that it is unable to calculate effective results using the ASTM D5617-04 stress calculation equation. The ratio of geotextile thickness to diameter is less than 0.1, so the stress problem of geotextile can be analyzed according to the thin-walled pressure vessel theory. The tensile stress formula derived from thin-film theory can avoid the thickness measurement problem in spherical bulge deformation under ring-restrained conditions, as shown in Eq. (1) [17]:

$$T = \frac{L}{8}\left(\frac{2H}{L} + \frac{L}{2H}\right)P, \tag{1}$$

where H is the sample's air expansion height (mm), and L is the inner diameter of the restrained ring. See Eq. (2) for strain calculation of geotextiles under multiaxial stretching conditions.

See Eq. (2) for strain calculation of geotextile under multiaxial tension (Li et al. 2016):

$$\varepsilon = \frac{L^2 + 4H^2}{4HL} \times \arccos\frac{L^2 - 4H^2}{L^2 + 4H^2} - 1, \tag{2}$$

where ε is the strain of geotextile during air expansion deformation, using the average strain on the spherical great circle curve through the apex of the spherical crown.

According to Eqs. (1) and (2), the tensile stress and strain of geotextiles with different diameters were calculated and plotted (Fig. 4).

Fig. 4 shows the typical tensile stress-strain relationship of geotextiles. The mechanical characteristic curve of 100 mm diameter can be divided into four stages: linear elastic stage, yield stage, strengthening phase, and failure stage. The mechanical characteristic curve of 200 mm can be divided into three stages: linear elastic stage, yielding stage, and failure stage, where the difference from that of 100 mm is that the linear elastic stage is steep, and the yielding stage produces strain softening and no strengthening phase. When starting to pressurize, the tensile stress on the geotextile increases rapidly; that is, the tensile stress between fibers gradually increases. The increased diameter greatly influences the tensile stress-strain formula in the early stage because the increased cavity space of the aperture leads to the uneven pressurization of the geotextile compared with the small aperture.

When the test area of geotextile and film increases, the film deforms greatly due to the high elongation of geotextile, and the strength produced by the film becomes high. In addition, considering that the strength of the geotextile itself is not high, which leads to a higher air expansion pressure in the initial stage of geotextile deformation, and finally manifests itself as a sharp increase in the linear elastic phase of the geotextile tensile stress-strain curve.

3.3. Test on influencing factors of geotextile bulge deformation

3.3.1. Influence of loading rate on spherical bulge deformation of geotextile

Seven loading rates of 80, 90, 100, 110, 120, 130, and 140 mL/min were adopted for the test. The variation of the geotextile deformation degree with the loading rate is shown in Fig. 3. Under the loading rate of 80 ml/min, the average bursting crown height is 77.12 mm, and the average bursting pressure is 1.46 MPa. The bursting crown height under 140mL/min is 1.07 times that of 80 L/min, and the bursting pressure is 0.837 times that of 80 L/min. It can be seen that there is a positive correlation between the bursting height of geotextiles and the loading rate; that is, the crown height increases with the increase of the loading rate until it bursts. The burst pressure is negatively correlated with the loading rate; that is, the bursting pressure decreases with the increase of the loading rate until it bursts.

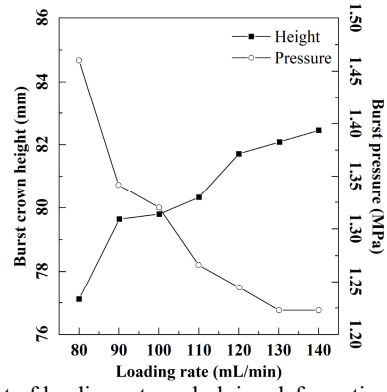

Fig. 3. Effect of loading rate on bulging deformation of geotextile

It can be seen from Fig. 3 that with the increase in loading rate, the change rate of bursting pressure and bursting crown height gradually decreases. When the loading rate is 130 mL/min-140 mL/min, the change rate of bursting pressure and bursting crown height is moderated that the amplitude of variation decreases, compared with the previous rates. Therefore,

a loading rate of 140 mL/min is selected as the basic loading rate for the subsequent tests, which could ensure that a larger bursting crown height could be achieved under a smaller bursting pressure and the shape of spherical bulging deformation and failure of the geotextile would be easier to observe.

3.3.2. Influence of restraint flange diameter on spherical bulge deformation of geotextile

The test was carried out with two inner diameters of 100 and 200 mm, and the variation of geotextile tensile stress-strain with the diameters can be seen in Fig. 4.

Results show that the expansion pressures of aperture 100 mm and 200 mm are about 1.05 MPa and 1.075 MPa, respectively, while the crown height is about 30 mm and 80 mm, respectively. The larger the aperture, the larger the burst crown height, and the higher the burst pressure during bulging deformation. Under the same condition, the deformation of the geotextile with a 100 mm diameter is more apparent. The change stage of the tensile stress-strain mechanical curve of geotextile with a 100 mm diameter is more comprehensive and the bulging deformation characteristics of geotextile can be reflected more clearly. That is why the restraint flange diameter of 100 mm is selected as the basic diameter for subsequent tests.

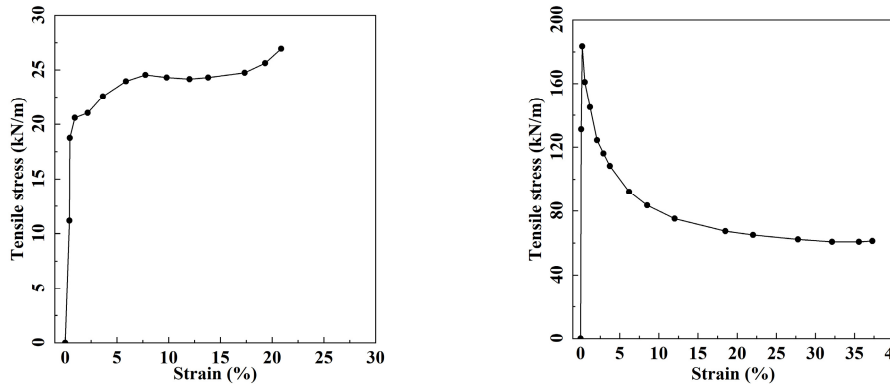

a) 100 mm b) 200 mm

Fig. 4. Tensile stress-strain curve of typical geotextile

3.3.3. Influence of material characteristics on spherical bulge deformation of geotextile

3.3.3.1. Influence of mass per unit area on bulge deformation of geotextile

The changes in the bursting pressure-crown height curve and tensile stress-strain curve of polyester staple geotextile with different unit area mass under the diameter of 100 mm are shown in Fig. 5.

The average burst crown height of 200 g/m^2 geotextile is 32.18 mm, and the average burst pressure is 1.07 MPa. Compared with the 200 g/m^2 geotextile, the average bursting crown height and the average bursting pressure of 400 g/m^2 geotextile increased by 23.06 % and 34.58 %, respectively. As the mass per unit area of geotextile increases, its bursting crown height and bursting pressure increase, and the increase of bursting pressure is more significant; The strain of 200 g/m^2 geotextile is 21.10 %, and the tensile stress is 27.04 kN/m. The strain of 400 g/m^2 geotextile is 29.93 %, and the tensile stress is 35.76 kN/m. When the strain exceeds 3 % in the figure, the stress-strain curve of the geotextile begins to have an obvious distinction. That the geotextile with a large mass per unit area has greater tensile stress at the same strain. When the mass per unit area increases, the fiber's density increases, the entanglement point's cohesive holding force grows, and its ability to resist deformation is strengthened.

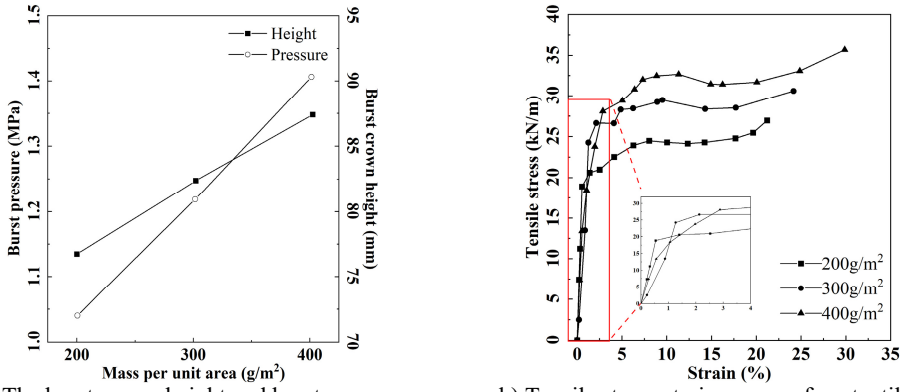

a) The burst crown height and burst pressure of geotextiles

b) Tensile stress-strain curves of geotextiles

Fig. 5. Influence of mass per unit area on bulging deformation of geotextile

3.3.3.2. Influence of fiber types on bulge deformation of geotextile

Under the diameter of 100 mm, the change of tensile stress-strain curve for the geotextile with different fiber types is shown in Fig. 6.

Fig. 6 shows that in the whole stage of bulging deformation, the tensile stress of polypropylene staple fiber geotextile is larger than that of polyester staple fiber geotextile at the same strain.

The test results show that the properties of polypropylene staple fiber geotextile are better than that of polyester staple fiber geotextile, indicating that polypropylene fiber strength is better than polyester fiber and polypropylene fiber has a higher initial modulus.

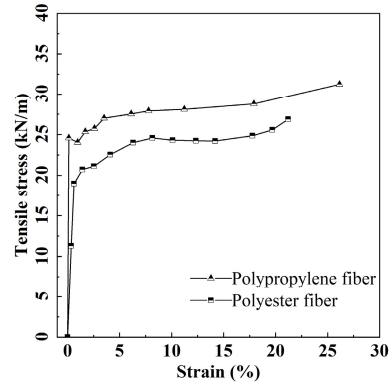

Fig. 6. Tensile stress-strain curves of geotextiles with different fiber types

3.3.3.3. Influence of fiber length on bulging deformation of geotextile

The tensile stress-strain curve for the bulging deformation of polyester filament and staple fiber geotextiles under the 100 mm diameter is shown in Fig. 7.

The difference in fiber length is that filaments are continuous fibers, while staple fibers range from a few millimeters to tens of millimeters. As shown in Fig. 7, in the initial stage of bulging deformation, the curve trends are similar, and the difference between the length of fibers is not obvious. With the increase of strain, the tensile stress of polyester filament geotextile is greater than that of polyester staple fiber geotextile at the same strain. The test results showed that the properties of polyester filament geotextile are better than that of polyester staple geotextile. That is, polyester filament geotextile has a stronger stress tolerance in the use process.

The increase in fiber length improves the probability of entanglement between fibers, not only

making the interlacing between fibers become tighter but also increasing the cohesive holding force at the entanglement point, which enhances the mechanical properties as well.

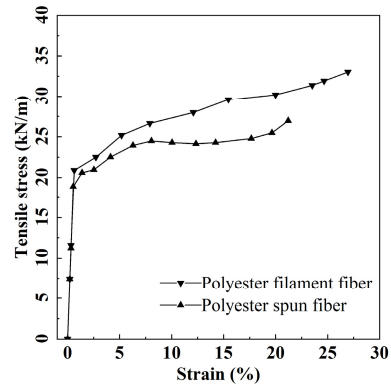

Fig. 7. Tensile stress-strain curves of geotextiles with different fiber lengths

3.4. Influence of geotextile on bulge deformation of geomembrane

If the new scheme of "cloth under and membrane over" is adopted in the test, due to the high permeability of the geotextile itself, pressure media such as water and air can directly exert pressure on the membrane through the cloth to make the membrane bulge. The geotextile under the membrane only plays a protective role, which does not affect the mechanical properties of the air expansion deformation.

Thus, it is easier for observing phenomena and recording data to cover the membrane with a cloth. The tests were carried out using the geomembrane, the geotextile, and the cloth covering the membrane. The changes in tensile stress-strain curves for the bulging deformation of three kinds of specimens under the diameter of 100 mm are shown in Fig. 8. The Influence of geotextile on the bulging deformation of the geomembrane is analyzed from three aspects-strength, deformation, and stress-strain. The crown height of the cloth covered on the membrane increased with the bulging pressure during the whole bulging test. At the initial stage of bulging deformation, the geomembrane was under great internal pressure. With the development of bulging deformation and the increase of crown height, the internal pressure borne by the geomembrane gradually decreases, while the internal pressure borne by the geotextile gradually rises to the main internal pressure, which plays a decisive role until it is destroyed. The bursting height of the cloth covering the membrane is slightly greater than that of a single geotextile, and its bursting pressure is close to the sum of geomembrane bursting pressure and geotextile bursting pressure, which is higher than that of a single geomembrane or geotextile, indicating that the bulging pressure it bears is shared by the membrane and cloth, respectively.

When the cloth is covered on the membrane, the failure order is the first geotextile, then the geomembrane. It will burst when the maximum deformation of the geotextile is reached.

At the same time, the geomembrane with larger deformation under the cloth is extruded from the burst place of geotextile and continues to bulge and deform until it breaks-the overall strength of the failure stage decreases, and the slope of the curve decreases. As long as the geotextile is damaged, its pressure is immediately borne by the membrane and quickly produces stress concentration, resulting in rapid destruction of the geomembrane. It can be seen from Fig. 8 that the overall trend of the bulging tensile stress-strain curve of cloth covering the membrane is similar to that of geotextile. It is divided into four stages: elasticity stage, yield stage, strengthening phase, and failure stage. Because of strain softening and other reasons, the single geotextile has a large yield degree. With the increase of deformation, the tensile stress decreases, and the strength declines. The geotextile strength is improved, which makes the tensile stress of the cloth covering the geomembrane is slightly larger than the sum of the two. With the increase of strain, the tensile

stress in the strengthening phase increases rapidly. The shape and slope of the curve are similar to those of the geotextile. Its magnitude is about the sum of the two, indicating that the two's joint action influences the bulging deformation in this stage. However, geotextile also mainly determines the deformation characteristics. When the cloth is covered on the membrane, the cloth not only protects the integrity of the geomembrane but also reduces the bulging deformation of the geomembrane so that its mechanical properties are enhanced compared with the bulging deformation of a single layer sample.

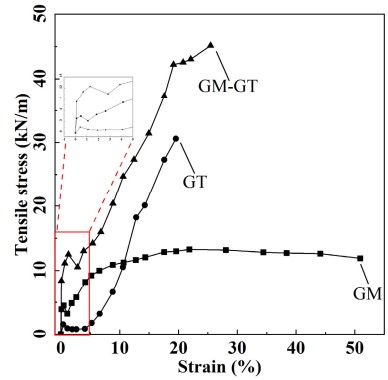

Fig. 8. Tensile stress-strain curves for bulge deformation of three samples

4. Conclusions

The following conclusions are drawn through the tests mentioned above and analytical discussions.

1) Under the ring-restrained conditions, the main factors affecting the geotextile's bulging deformation are the equipment's loading rate, the inner diameter of the restraint flange, and the material characteristics of the geotextile. The tensile stress-strain curve of geotextile bulging deformation can be divided into four stages: elastic stage, yield stage, strengthening phase, and failure stage.

2) The average burst crown height of 200 g/m^2 geotextile is 32.18 mm, the average burst pressure is 1.07 MPa, the strain is 21.10 %, and the stress is 27.04 kN/m. The appearance of its bulging deformation is similar to a spherical crown, and the failure mechanism is that the fiber nodes in the needle punching direction of the weak area of the crown break away from failure, and the fiber perpendicular to the needle punching direction tears. The failure mode is progressive tearing, and the damage shape is approximately spindle-shaped.

3) With the increase of loading rate, the bursting crown height of geotextile increases and the bursting pressure decreases, but the decreasing amplitude gradually reduces; The bursting crown height and bursting pressure increase with the increase of diameter.

4) The burst pressure and burst crown height of the geotextile have an approximately linear relationship with the mass per unit area. Moreover, increase with the mass per unit area, but the magnitude of increase in bursting crown height is relatively small, which indicates that the geotextile has stronger resistance to deformation. The fiber type and length impact the burst crown height and burst pressure of the geotextile, and the mechanical properties of the polypropylene fiber geotextile are better than that of the polyester fiber geotextile. The more extended the fiber length is, the stronger the mechanical properties of geotextile are.

5) When the cloth is covered on the membrane, the bulging pressure it bears is shared by the membrane and cloth, respectively, and they are destroyed successively. Compared with a single geomembrane, the bursting stress is increased by 114 %, while the strain is reduced by 11 %, reducing the geomembrane's bulging deformation to some extent. The mechanical properties are enhanced compared to the single sample, but the geotextile determines the deformation properties.

Acknowledgements

This work was financially supported by the Shandong Provincial Natural Science Foundation, China (ZR2019MEE106).

Data availability

The datasets generated during and/or analyzed during the current study are available from the corresponding author on reasonable request.

Author contributions

Zhe Yang: Methodology, Software, writing – original draft preparation and writing – review and editing; Wanglin Li: project administration and supervision, conceptualization, funding acquisition, resources and validation; Xia Xue: formal analysis and data curation; Chen Li: investigation and methodology.

Conflict of interest

The authors declare that they have no conflict of interest.

References

[1] J. P. Yuan et al., "Field Test study of mechanism of bulge phenomenon under geomembrane in plain reservoir," (in Chinese), *Rock and Soil Mechanics*, Vol. 35, No. 1, pp. 67–73, 2014.

[2] D. C. Ren et al., "Testing techniques and functional mechanism of composite geomembranes," (in Chinese), *Chinese Journal of Geotechnical Engineering*, Vol. 20, No. 1, pp. 10–13, 1998.

[3] H.-R. Yu, W.-L. Li, R.-C. Wei, and C. Li, "Experimental study on air expansion deformation of composite geomembrane under ring-restrained condition," (in Chinese), *Geotechnical Testing Journal*, Vol. 43, No. 5, pp. 20180381–1200, Sep. 2020, https://doi.org/10.1520/gtj20180381

[4] Y. C. Pu et al., "Effect of combination modes of geomembrane and geotextile on bulging deformation of separated composite geomembrane," (in Chinese), *Journal of University of Jinan Science and Technology*, Vol. 34, No. 6, pp. 548–553, 2020.

[5] S. Dickinson and R. W. I. Brachman, "Assessment of alternative protection layers for a geomembrane – geosynthetic clay liner (GM-GCL) composite liner," *Canadian Geotechnical Journal*, Vol. 45, No. 11, pp. 1594–1610, Nov. 2008, https://doi.org/10.1139/t08-081

[6] J. R. Carneiro, P. J. Almeida, and M. L. Lopes, "Evaluation of the resistance of a polypropylene geotextile against ultraviolet radiation," *Microscopy and Microanalysis*, Vol. 25, No. 1, pp. 196–202, Feb. 2019, https://doi.org/10.1017/s1431927618000430

[7] J.-C. Hsieh, J.-H. Li, C.-H. Huang, C.-W. Lou, and J.-H. Lin, "Statistical analyses for tensile properties of nonwoven geotextiles at different ambient environmental temperatures," *Journal of Industrial Textiles*, Vol. 47, No. 3, pp. 331–347, Sep. 2017, https://doi.org/10.1177/1528083716647199

[8] T. L. Andrejack and J. Wartman, "Development and interpretation of a multi-axial tension test for geotextiles," *Geotextiles and Geomembranes*, Vol. 28, No. 6, pp. 559–569, Dec. 2010, https://doi.org/10.1016/j.geotexmem.2010.04.001

[9] S. Chen, X. Ding, R. Fangueiro, H. Yi, and J. Ni, "Tensile behavior of PVC-coated woven membrane materials under uni – and bi-axial loads," *Journal of Applied Polymer Science*, Vol. 107, No. 3, pp. 2038–2044, Feb. 2008, https://doi.org/10.1002/app.27303

[10] S. M. Merry and J. D. Bray, "Geomembrane response in the wide strip tension test," *Geosynthetics International*, Vol. 3, No. 4, pp. 517–536, Jan. 1996, https://doi.org/10.1680/gein.3.0073

[11] H. Pincus, S. Merry, J. Bray, and P. Bourdeau, "Axisymmetric tension testing of geomembranes," *Geotechnical Testing Journal*, Vol. 16, No. 3, pp. 384–392, 1993, https://doi.org/10.1520/gtj10059j

[12] J. D. Bray and S. M. Merry, "A comparison of the response of geosynthetics in the multi-axial and uniaxial test devices," *Geosynthetics International*, Vol. 6, No. 1, pp. 19–40, Jan. 1999, https://doi.org/10.1680/gein.6.0141

[13] J. Pan, "Researches on characteristic geomembrane with damnification and applications," (in Chinese), Hohai University, 2002.

[14] C. Y. Chu and Y. X. Zhang, "Dynamic creep and fatigue properties of geotextiles," (in Chinese), *Journal of Textile Research*, No. 1, pp. 33–35, 2002.

[15] "Standard test method for bursting strength of textile fabrics-diaphragm bursting strength tester method," ASTM D3786/D3786M-18(2018), ASTM International, 2018.

[16] "Textiles – Bursting properties of fabrics – Part 1: Hydraulic method for determination of bursting strength and bursting distension," ISO 13938-1(2019), Geneva, Switzerland, International Organization for Standardization, 2019.

[17] W. L. Li et al., "Experimental study on air expansion deformation of geomembrane under ring-restrained conditions," (in Chinese), *Chinese Journal of Geotechnical Engineering*, Vol. 38, No. 6, pp. 1147–1151, 2016, https://doi.org/10.11779/cjge201606023

Zhe Yang is a master's degree and studying in water conservancy project of University of Jinan.

Xia Xue is a Ph.D. student and studying in water conservancy project of University of Jinan.

Wanglin Li received Ph.D. degree in College of Water Conservancy and Hydropower Engineering from Hohai University, Nanjing, China, in 2006. Now he works at University of Jinan. His current research interests include hydraulic structure and geosynthetics.

Chen Li received Master degree in College of Water Resources and Environment from University of Jinan, Jinan, China, in 2020. Now he works at Shandong Water Conservancy Engineering Test Center Co., Ltd.